Population dynamics of generalist/specialist strategies in the feast-famine cycle

Rintaro Niimi[1], Chikara Furusawa[2,3], Yusuke Himeoka[2]

1 Department of Biological Sciences, Graduate School of Science, The University of Tokyo, Bunkyo-ku, Tokyo, Japan
2 Universal Biology Institute, Graduate School of Science, The University of Tokyo, Bunkyo-ku, Tokyo, Japan
3 Center for Biosystems Dynamics Research, RIKEN, Chuo-ku, Kobe, Japan

Abstract

Microbial populations exhibit a broad spectrum of nutrient utilization strategies, ranging from strategies utilizing diverse nutrients, called "generalist," to ones being highly adapted to specific nutrients, called "specialists." The mathematical conditions for the diversification of nutrient utilization strategies are central questions in theoretical ecology. Previous studies have shown that trade-offs among different resource utilization functions that cells cannot utilize broad types of substrates at near-maximum speed are crucial for the emergence of diverse strategies. However, in natural settings, nutrient availability often fluctuates over time, imposing additional trade-offs on cells. Cells that grow rapidly under nutrient-rich conditions will suffer a higher death rate under nutrient-poor conditions, creating a growth-death trade-off that intersects with the classical resource-use trade-off. Here, we introduce a unified mathematical model that simultaneously incorporates the resource-use trade-off and the growth-death trade-off. The nutrient supply was modeled as discrete stochastic events, capturing realistic temporal fluctuations. We show that the relative balance between growth and death rates critically influences the dominance of either generalist or specialist strategies. Specifically, under conditions of high average growth rates among different environments and a weak trade-off between growth and death rates, generalists prevail. In contrast, when the growth-death trade-off is intense, specialists emerge as the dominant strategy. Our findings reveal that accounting for the growth-death trade-off is crucial for understanding how microbial communities adapt and evolve in temporally varying environments.

Author summary

Microbial strategies for choosing which nutrients to utilize are highly diverse. In our study, we explored why some microbes become generalists able to use a variety of nutrients, while others specialize in only a few nutrients. These strategies are often considered to result from metabolic trade-offs during nutrient processing. However, in fluctuating environmental conditions, it is important to consider additional trade-offs; in nutrient-rich conditions, they can grow quickly, but this often comes at the cost of being more vulnerable when nutrients are scarce. To investigate how these trade-offs affect the emergence of generalists and specialists, we developed a simple model that mimics the natural cycles of plenty and scarcity of nutrients, which is called the

feast-famine cycle. Our work shows that the trade-off between growth and death rates is crucial for determining whether a generalist or specialist strategy dominates. We highlight the importance of trade-offs in the response to environmental changes in shaping microbial adaptive strategies.

Introduction

Microbes are the most abundant and diverse organisms on Earth [1], inhabit a wide range of environments and form the fundamental basis of ecosystems [2]. Despite their diversity in the wild, the mechanisms that enable the stable coexistence of multiple microbial species remain an open question in mathematical ecology. Classical theories argue that increasing species diversity within an ecosystem tends to reduce stability, making the coexistence of species in a single habitat difficult. According to the classical interpretation of Gause's competitive exclusion principle, species competing for the same resources cannot coexist and eventually lead to the dominance of a single species, driving others to extinction [3, 4]. Resolving such discrepancies between theories and observations in the wild has been one of the central questions in the mathematical ecology field [5].

One key factor that facilitates species coexistence is the differentiation in nutrient utilization [5]. In the wild, nutrients for microbial cells are present in the form of complex molecules, not just as, a specific carbon source, such as glucose. These complex molecules may provide various carbon sources and amino acids. By utilizing different nutrients, species can avoid competition, enabling the stable coexistence of multiple species within the same habitat [6, 7].

What drives segregation of nutrient utilization by different microbial species? Why do no species monopolize all nutrients? Trade-offs are known to play a pivotal role [8]. In laboratory experiments, microbes often exhibit trade-offs in their ability to utilize different nutrients, such as the trade-off between fructose and galactose [9], silicon and phosphorus [10], and nitrogen and phosphorus [11]. When cells enhance their ability to utilize one nutrient, the utilization of other nutrients is constrained, which promotes differentiation of resource use among species. These trade-offs stem from various functional constraints on cellular metabolism, one of which is the limited capacity of protein abundance. A well-established view of the proteome partitioning [12, 13], cells cannot activate all metabolic pathways at the maximum speed at the same time. The cells have to decide which pathway to activate by sacrificing the capacity to utilize other nutrients [14]. Additionally, there are constraints due to the thermodynamic nature of metabolism. For instance, glycolysis and gluconeogenesis share several metabolic reactions, whereas the two metabolic pathways proceed in opposite direction. This makes the simultaneous utilization of the glycolytic- and gluconeogenic carbons infeasible [9, 15].

The presence of such inherent trade-offs compels microbes to choose which nutrient to utilize and may lead to a variety of nutrient-utilization strategies. The two extremes of nutrient utilization strategies are so-called *generalists* and *specialists*. Generalists can adapt to diverse conditions, while the utilization speed and/or efficiency of nutrients is typically lower than that of other strategies. Specialists can utilize only a limited number of nutrients while thriving in adapted nutrient conditions [16, 17]. Experimental and theoretical studies have provided several pieces of evidence that the emergence of diverse nutrient utilization strategies is instrumental in promoting ecosystem diversity [18–20].

Another key aspect of the emergence of diverse ecosystems is the change in environmental conditions over time [21–25]. Temporal changes in nutrient availability are one of the main driving forces behind ecosystem dynamics. In natural

environments, particularly in ecosystems such as lakes, the surface layer of oceans, and soils, nutrients are not continuously supplied as in chemostats, but are instead supplied in discrete and stochastic events. Once nutrients are supplied, the ecosystem experiences a period of feast, but such a delightful time ends by eating up nutrients, leading to famine. This alteration in environmental conditions is known as the feast-famine cycle [26–29].

Under feast-famine conditions, cells must find a way to survive the famine period by dealing with several stresses, such as starvation. They can increase survivability under stressful conditions by producing stress response proteins at the expense of growth, by reducing the production of cell growth-associated proteins [12, 30]. For instance, *rpoS*, which encodes a sigma factor, is one of the key regulatory genes involved in the regulation of *E. coli*. Deletion mutants lacking *rpoS* showed higher growth but reduced stress resistance [31]. Although stress responses require remodeling of the proteome profile of the cell, proteome remodeling under starved conditions is another challenge; for remodeling the proteome profile, degradation of existing proteins and synthesis of new proteins are necessary, both of which are energy-demanding processes. In particular, in bacterial cells, protease activity is lower than that in eucaryotic microbes [32]; thus, dilution by the volume growth of the cell is the main process of decreasing protein concentration. Proteome profile remodeling demands resource-fueled cellular activity, and thus, it is challenging to carry out it as an immediate response to the depletion of nutrients [33, 34]. To cope with such circumstances, microbes are known to have basal expression of stress response genes even under growing conditions [35]. This "safety" is at the expense of the growth rate, and indeed leads to the trade-off between the growth rate and the death rate [34].

How do these two trade-offs orchestrate and drive the diversity of nutrient utilization strategies? To date, the trade-off between the range of utilizable nutrients and the growth rate has been actively investigated and is considered one of the key factors of whether a generalist-like or a specialist-like strategy will have a higher advantage in a given environment; if strong trade-offs exist, where adaptation to one resource use significantly hampers the use of the other, specialists tend to evolve, and *vice versa* [14, 36, 37]. Only with such a trade-off does the strength (i.e., the functional form of the trade-off), determine the fittest strategy. In this sense, the environmental conditions, such as the amount of nutrients and frequency of the supply have no impact on the emergence of the different nutrient utilization strategies. Variations in nutrient availability and supply regimes strongly influence community composition and ecosystem processes in tropical ecosystems [38], indicating that the assumption of optimal strategies dictated solely by the functional form of trade-offs may be divorced from ecological reality. Henceforth, we examine the influence of two trade-offs—the trade-off between the range of utilizable nutrients and the growth rate, and the growth-death trade-off on the emergence of the multiple nutrient utilization strategy.

To determine how the resource-use trade-off and the growth-death trade-off synergistically affect nutrient utilization strategies, we constructed a population dynamics model of multiple phenotypes and nutrients exhibiting feast-famine cycle dynamics. In this model, nutrients are supplied by discrete and stochastic events that initiate the feast period. Once the feast period begins, the cells consume nutrients, leading to famine. We introduce two types of trade-offs for the microbes: if a phenotype wants to utilize a wide variety of nutrients, it cannot show the growth as rapid as another phenotype that grows only on a limited number of nutrient sources. In addition, if a phenotype has a higher growth rate during the feast period, it shows a higher death rate under famine conditions.

Using this model, we showed that either a generalist or specialist strategy can be dominant in the population, depending on environmental conditions. The transition of

the fittest strategy from specialists to generalists occurred when the maximum average growth rate increased beyond the critical value, and the transition of the optimal strategy was triggered by the strength of the trade-offs. Our results provide insights into possible mechanisms of diversification of resource use strategies in temporally varying environments, which is more typical in the wild than in chemostat conditions. We also discuss the impact of fluctuations in nutrient supply intervals on nutrient utilization strategies.

Model

In the present study, we investigated the influence of trade-offs on the emergence of nutrient usage strategies. For this purpose, we considered the population dynamics of microbes in the feast-famine cycle. In the following, we use the term "phenotype" instead of species because different phenotypes differ only in their nutrient-utilization strategy.

The model consists of N phenotypes. Nutrients are supplied to the environment as a discrete stochastic event, while the population growth of the phenotypes is modelled using continuous-time deterministic ordinary differential equations. Here, we consider that there are multiple types of nutrients, such as different carbon sources. There are E types of nutrient sources and one type of nutrient is supplied by a single supply event. As will be seen, the supplied nutrient is typically consumed much earlier than the next supply event, and thus, at most one type of nutrient is present in the system simultaneously. Hence, the type of nutrient supplied at the latest supply event sets the environmental condition; thus, we represent the environmental condition by the type of nutrient at the latest supply. Since the cells regulate the intracellular state to utilize the supplied nutrients, the environmental conditions set the growth rate and death rate of the cells. We denote the growth rate and death rate of phenotype i in environment e by $\mu_{i,e}$ and $\gamma_{i,e}$, respectively. The model equation for the population of phenotype i, X_i, is as follows:

$$\frac{dX_i}{dt} = \begin{cases} \left(1 - \sum_{i \neq j} A_{i,j}\right) \mu_{i,e} X_i + \sum_{i \neq j} A_{j,i} \mu_{j,e} X_j & (S > 0) \\ -\gamma_{i,e} X_i & (S = 0) \end{cases} \tag{1}$$

$$\frac{dS}{dt} = -\sum_{i=1}^{N} \mu_{i,e} X_i$$

where S is the amount of nutrient. For simplicity, we assumed that the amount of nutrients was set to the type-independent value S_0 at the supply event. As the type of supplied nutrient is encoded in the growth and death rate, we omit the subscript on S to denote the type of nutrient and only represent the amount. In the current setup, it is not possible for more than two types of nutrients to be present simultaneously, that is, leftover nutrients are not allowed. The following results are not affected if we generalize the setup so that the nutrients can be left unconsumed because the cells are greedy enough to eat up nutrients before the next supply event.

During the feast ($S > 0$) period, cells grow and proliferate at a rate $\mu_{i,e}$. During the division event of a cell of the ith phenotype, we allow the daughter cell to have the jth phenotype with probability A_{ij}. However, during the famine ($S = 0$) period, the cells die at rate $\gamma_{i,e}$. While we adopt a differential equation framework to describe continuous-time population dynamics, we incorporate the discreteness of the population by introducing a threshold θ below which populations are set to zero.

Nutrient supply events occur at random and discrete time points τ_k $(k = 1, 2, \ldots)$. At each event, the amount of nutrient S discontinuously jumped to a constant value S_0.

$$S(\tau_k) = S_0 \tag{2}$$

The type of supplied nutrient, that is, the environmental index e, was randomly chosen for the nutrient supply event τ_k (Fig 1).

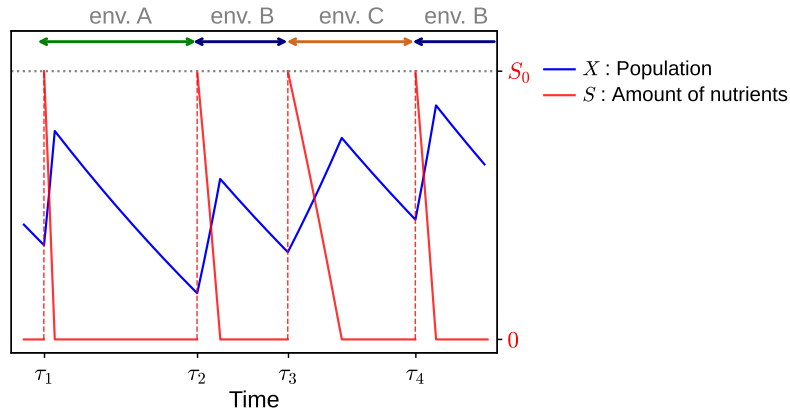

Fig 1. Schematic of the population dynamics model. Temporal changes in population size and nutrient levels. The blue line represents the population X, and the red dashed line represents the amount of nutrients S. At the certain time point $\tau_1, \tau_2, \cdots$, nutrients are supplied and S is set to S_0. At each time τ_k, a different type of nutrition is randomly selected and supplied. The type of nutrients supplied depends on the value of environmental variables. Here, we have only a single phenotype and the growth rates are set such that $\mu_A > \mu_B > \mu_C$.

In this model, we introduced two types of trade-offs. The first trade-off is the resource use trade-off. In situations where different nutrients come alternately, cells can partially compensate for the trade-offs imposed by metabolic constraints by transcriptionally reorganizing their proteome. However, this requires cells to constitutively maintain additional nutrient-sensing and catabolic proteins, which incurs a growth cost [39, 40]. Consequently, cells still face an inherent resource-use trade-off of different nutrient utilization even under conditions of alternating nutrient supplies.

Here, we assumed that there is a strong trade-off in the cost of utilizing different nutrients. The second derivative of the trade-off function (d^2y/dx^2) is often used as a measure of the strength of trade-offs [14, 36, 37]. When the trade-off function is convex $(d^2y/dx^2 > 0)$, the acquisition of both traits is more restricted than in the marginal, linear trade-off case $(d^2y/dx^2 = 0)$. Therefore, this is referred to as a strong trade-off. However, when the trade-off function is concave $(d^2y/dx^2 < 0)$, it is called a weak trade-off. According to Caetano et al., there is no room for nutrient utilization strategy to diversify with concave trade-offs [14]. Thus, we introduced the convex trade-off among the growth rates in different nutrients using the following function, while the specific choice of the function did not alter the result (see SI for details):

$$\left(\prod_{e=1}^{E} \mu_{i,e} \right)^{\frac{1}{E}} = \bar{\mu} \tag{3}$$

In addition to the above trade-off (Eq (3)), we introduce a trade-off between growth rates and death rates. In a study by Biselli et al. [34], the authors cultured $E.$

coli cells in several media containing a single carbon source, and then the cells were washed and transferred into a carbon-free buffer medium to examine the relationship between the growth rate under nutrient-rich conditions and the death rate during the subsequent starvation state. They reported that the death rate in a carbon-free buffer medium increases exponentially with growth rate under nutrient-rich conditions. This relationship was generic among the different carbon sources in the medium. According to this result, we introduce an exponential trade-off between the growth rate and the death rate as follows:

$$\gamma_{i,e} = a \cdot \exp(b\mu_{i,e}), \tag{4}$$

where a and b are constant values independent of i and e, respectively.

Results

Generalist-dominance and Specialist-dominance

The purpose of the present study was to identify the conditions that set the optimal nutrient utilization strategies. As an initial step for answering such a question, we start with a simple model, where the model equation consists of $N = 3$ phenotypes and $E = 2$ environmental conditions. We index the phenotypes by Arabic numbers (phenotypes 1, 2, and 3) and environments by alphabet (environments A and B).

In the present simple model, we set the growth rates of phenotypes in ascending and descending order, that is, the growth rate in environment A follows $\mu_{1,A} > \mu_{2,A} > \mu_{3,A}$ and that in environment B follows $\mu_{1,B} < \mu_{2,B} < \mu_{3,B}$. To begin with the simple case, we assume the symmetry between environments A and B by $\max_i \mu_{i,A} = \max_i \mu_{i,B}$ and $\min_i \mu_{i,A} = \min_i \mu_{i,B}$. One way to implement this symmetry with consistency with the resource-use trade-off (Eq (3)) is as follows:

$$\mu_{1,A} = 2\bar{\mu}, \mu_B = \bar{\mu}/2, \mu_{2,A} = \mu_{2,B} = \bar{\mu}, \mu_{3,A} = \bar{\mu}/2, \mu_{3,B} = 2\bar{\mu}$$

Because of this growth rate setting, phenotype 2 has a generalist-like strategy, where the growth rates are the same in the two environments, while the other phenotypes are specialist-like compared to phenotype 2. Note that the two specialists can also grow under environmental conditions in which the phenotypes have a lower growth rate; therefore, they are not extreme specialists that cannot grow under certain environmental conditions.

We assumed that the choice of nutrient-utilization strategy did not affect the probability of phenotypic switching. In addition, the phenotypic switch is considered to occur only in the nearest neighbor of the phenotype index. Overall, the phenotype switching probabilities are given by

$$A_{ij} = \begin{cases} p & (|i-j| = 1) \\ 0 & (otherwise) \end{cases} \tag{5}$$

We also assumed that the waiting time for nutrient supply events, $\Delta\tau_k$ follows a gamma distribution. The gamma distribution is a generalized form of the Erlang distribution that is widely employed to describe the queuing time distribution of events that follow the Poisson process.

Fig 2 shows the population dynamics in two different simulation setups, $\bar{\mu} = 0.4$ and 0.8. We observed two distinct types of population dynamics: in the first case, the two specialist phenotypes dominated the community (Fig 2A), and in the second case, the generalist phenotype became dominant (Fig 2B). This result was also observed

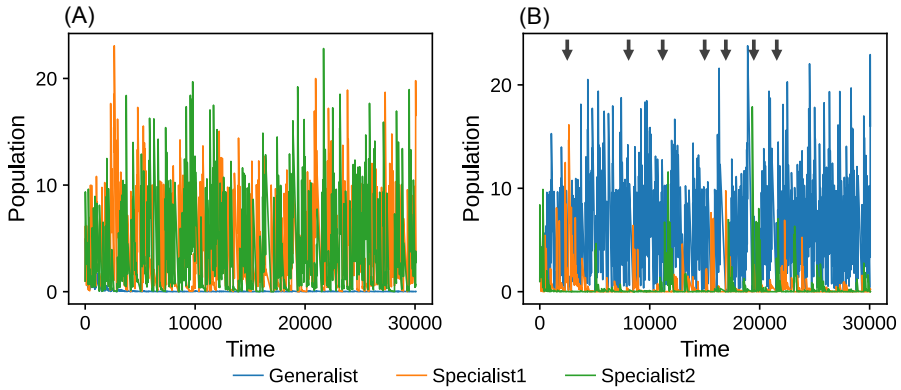

Fig 2. Examples of the simulation with $N = 3$ and $E = 2$. (A) The case with $\bar{\mu} = 0.4$. Two specialists dominate the population. (B) The case with $\bar{\mu} = 0.8$. The generalist dominates the population. The initial values of populations are set to unity for all three phenotypes. The parameters are set to $a = 0.01, b = 1, S_0 = 10, p = 10^{-4}$, and $\theta = 10^{-8}$. The waiting time for the nutrient supply $\Delta\tau_k$ $(= \tau_{k+1} - \tau_k)$ is sampled from the gamma distribution with shape and rate parameters being 2 and 50, $\Delta\tau_k \sim \Gamma(2, 50)$.

when the nutrient supply events occurred at regular intervals $\Delta\tau_k = \Delta\tau = \text{const.}$ for $k \geq 1$ (S1 Fig.).

To understand why the dominant phenotypes changed depending on the parameter value $\bar{\mu}$, we simulated the model with various values of $\bar{\mu}$. In this simulation, we set the intervals between successive nutrient supply events $\Delta\tau_k$ for $k \geq 1$ constant to clarify the effect of the parameter value on population dynamics. Fig 3A shows the temporal average of the population of the generalist and two specialists. The temporal average of the two specialists was taken, and the mean of the two averages is plotted in the figure. The generalist is dominant for a larger $\bar{\mu}$, and the specialists are dominant for a smaller $\bar{\mu}$.

To elucidate the mechanism of the transition between generalist and specialists dominance, we introduce a simple dimensionless parameter given by $r = \langle\mu\rangle/\langle\gamma\rangle$, where $\langle\mu\rangle$ and $\langle\gamma\rangle$ are given by $\langle\mu\rangle = (\mu_A + \mu_B)/2$ and $\langle\gamma\rangle = (\gamma_A + \gamma_B)/2$, respectively. Because the two specialist phenotypes exhibited symmetric growth properties with respect to the two environments $(\mu_{1,A} = \mu_{3,B}, \mu_{1,B} = \mu_{3,A})$, the values of r for the two specialists were the same. We denote the r values of specialists and generalists as r_s and r_g, respectively. The ratio of r_g to r_s is used as the horizontal top axis in Fig 3A. The figure shows that the transition between generalist- and specialist-dominant dynamics occurred at the value of r_g/r_s being unity. We carried out the same analysis by simulating the population dynamics by changing b value, which represents the strength of the growth-death trade-off (S2 Fig. A). As shown in Fig 3A, the transition occurred at the same value of r_g/r_s. The value of r_g/r_s at the transition point is robust to the parameter values of the phenotype switching probabilities p (S3 Fig.). The transition of dominant phenotypes is well captured by the ratio of the r-value between the generalist and specialists.

To determine why the ratio r_g/r_s determines the dominant phenotypes, we analytically estimated the transition point(see SI for details). Here, we examine the stability of the generalist or specialists dominating stability by calculating the

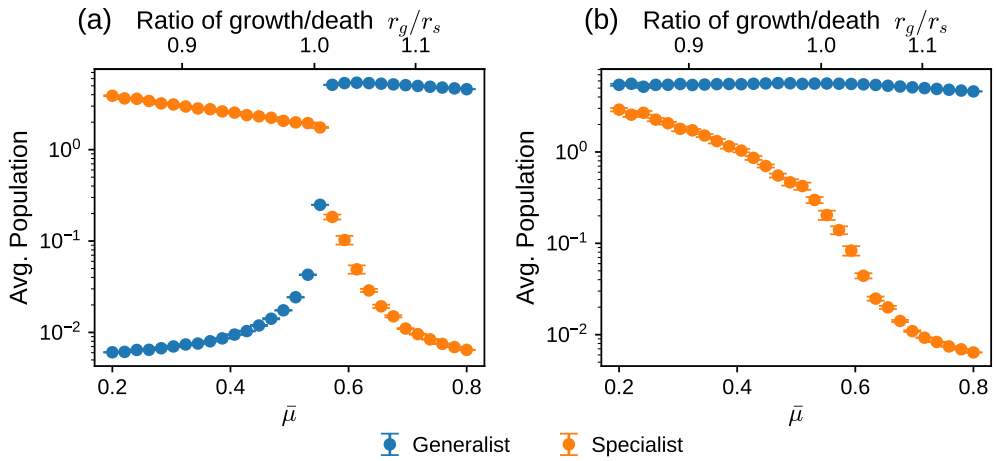

Fig 3. Temporal average of the population with constant $\Delta\tau$. The average population numbers are shown as a function of the parameter $\bar{\mu}$. The model with one generalist and two specialists is simulated for (A), while there is only a single specialist adapted to environment A for (B). We simulated up to $t = 3.0 \times 10^5$ and averaged the populations after $t = 2.5 \times 10^5$. For each $\bar{\mu}$, we ran 10 simulations and calculated the average population. The error bar indicates the standard error. The secondary x-axis shows the ratio of r_g to r_s. Throughout the simulations, the strength of the growth-death trade-off was fixed at $b = 1$, and nutrient supply events occurred at constant intervals ($\Delta\tau = 100$). All other parameters were identical to those used in Fig. 2.

invasibility of the other phenotype. We examined the invasibility of a mutant phenotype introduced at a low frequency. We demonstrated that the invasive phenotype can be fixed when the ratio of the growth rate to the death rate is larger than that of the pre-existing phenotype.

Given that r is defined as the ratio of the arithmetic mean of growth rate across the two environments to the arithmetic mean of death rate across the two environments, we therefore perform our analysis in a single, "averaged" environment by substituting μ and γ with their respective arithmetic means across the two environments. Phenotype i has a single averaged growth rate μ_i and death rate γ_i defined as follows:

$$\mu_i = \frac{\mu_{i,A} + \mu_{i,B}}{2}, \gamma_i = \frac{\gamma_{i,A} + \gamma_{i,B}}{2} \tag{6}$$

To determine each phenotype's capacity to persist and invade under time-varying resource availability, we summarized its overall population change across a single feast-famine cycle by net log growth between two consecutive nutrient supply events. The net log growth of phenotype i, f_i is given by

$$f_i = \mu_i T^+ - \gamma_i(\Delta\tau - T^+) \tag{7}$$

where T^+ is the duration of nutrient availability after the nutrient supply event. If f_i is positive, the population size increases; if f_i is negative, the population size decreases. When there is only a single phenotype (phenotype α), the population size settles at the point where $f_\alpha = 0$. Here, we considered the invasibility of an other phenotype (phenotype β). Phenotype β can be fixed when f_β is positive. Because phenotype β is a mutant phenotype introduced at a low frequency, the number of phenotype β is sufficiently small, and thus the change in the value of T^+ is negligible.

Because the value of T^+ satisfies $f_\alpha = 0$,

$$T^+ = \frac{\gamma_\alpha}{\mu_\alpha + \gamma_\alpha} \Delta\tau \tag{8}$$

Thus, f_β is given by

$$f_\beta = \frac{\gamma_\alpha}{\mu_\alpha + \gamma_\alpha} (\mu_\beta \gamma_\alpha - \mu_\alpha \gamma_\beta) \tag{9}$$

Therefore, phenotype β can invade if $\mu_\beta/\gamma_\beta > \mu_\alpha/\gamma_\alpha$ holds.

Interestingly, the transition did not occur in a simulation with one type of specialist and one type of generalist ($N = 2, E = 2$, phenotype 3 excluded) (Fig 3B and S2 Fig. B). In such cases, a generalist always dominates the system, and thus, the transition from generalist dominance to specialist dominance takes place through the cooperation of specialists to suppress the increase in the generalist population.

Thus far, we have set the waiting time for nutrient supply $\Delta\tau$ to be constant to analyze the deterministic effect of $\bar{\mu}$ and b on population dynamics. Next, we explore the effect of the randomness of waiting time on population dynamics. Fig 4 shows the temporal average of the population of the generalist and the specialists, where $\{\Delta\tau_k\}_{k\geq 1}$ follows a gamma distribution. The average population of specialists tended to be higher than that of the constant $\Delta\tau$ in the generalist-dominant region. The average population increase was also observed in the generalists, although the increase was less than that in the specialists.

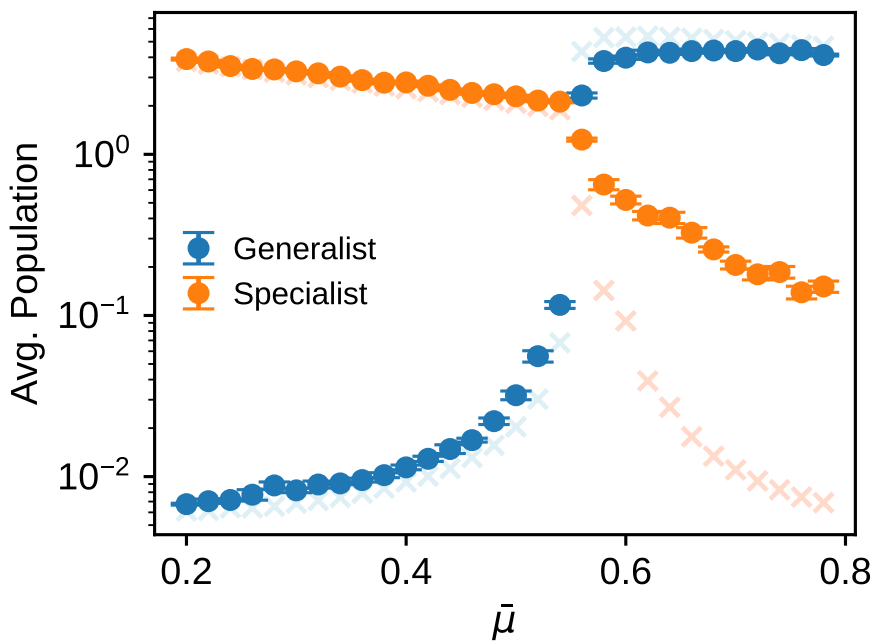

Fig 4. Temporal average of the population with random $\Delta\tau$. Changes in the average populations as the parameter $\bar{\mu}$ is varied in simulation with one generalist and two specialists. The waiting time for the nutrient supply $\{\Delta\tau_k\}_{k\geq 1}$ are sampled from a gamma distribution, $\Delta\tau_k \sim \Gamma(2, 50)$. We simulated up to $t = 3.0 \times 10^5$ and averaged the populations after $t = 2.5 \times 10^5$. For each $\bar{\mu}$, we ran 10 simulations and calculated the average population. The error bars indicate the standard error. We also display the results of $\Delta\tau = 100$ (Fig. 3A) in the background (cross marks).

We performed simulations under uniform and normal distributions, as well as the gamma distribution. In all cases, we observed an increase in the temporal average population of specialists compared with when $\Delta\tau$ was constant. As the variance of the distribution increases, the temporal average population also increases.

A possible explanation for the increase in the temporal average population of specialists is the long famine period. Once long waiting times for nutrient supply occur, the population decreases significantly. In such cases, the number of specialists who can grow faster than generalists can temporarily increase significantly.

In the present simulation, we studied a simple model with one generalist phenotype and two specialist phenotypes. Phenotype switching changes the growth rate by one to 2-fold and the other by 1/2-fold. Switching occurred among the three discrete phenotypes. However, in natural evolutionary processes, the mutational effects are typically gradual and continuous. To ensure that our findings are not an artifact of the limited number of phenotypes, we repeated the simulations with a finer discretization of phenotypes where growth rates vary smoothly along the constraint surface $\sqrt{\mu_{i,A}\mu_{i,B}} = \bar{\mu}$ (see the next section for details). This refined setting yielded a similar outcome: the system still underwent shifts in dominance between generalist and specialist strategies. Hence, the conclusions reported here are robust to the granularity of the phenotypic space.

Diversification of nutrient utilization strategies in multiple Environmental conditions

In this section, we increase the number of environmental conditions ($E = 3$ and 4) and observe their dynamics. In natural habitats, there are usually more than two available nutrients, and cells face a resource-use trade-off among multiple nutrients. Under these multi-nutrient conditions, not only two distinct strategies, generalist and specialist, but also a wider range of intermediate phenotypes can be observed. To capture the wider spectrum of possible nutrient utilization strategies, we introduced a more continuous phenotype space, where growth rates vary smoothly in the constraint defined by Eq (3).

First, to observe how a finer phenotype resolution alters outcomes compared to the discrete two-environment simulations in the previous section, we conducted simulations for two environmental conditions with an increased number of phenotypes ($N = 51$), refining the bins of the phenotype space. As in the simulations with one generalist and two specialists, we set the growth rates of phenotypes in ascending and descending order, and we suppose the symmetry between environments A and B. We set the growth rate of phenotype i as follows, which is consistent with the resource-use tradeoff.

$$\mu_{i,A} = \bar{\mu} \cdot g_i,\ \mu_{i,B} = \bar{\mu}/g_i,\ g_i = g^{(0)} \cdot m^{c \cdot i} \tag{10}$$

$\Delta\tau$ was set to a constant value, and the environment changed in deterministic order. Starting from an initial state where only a generalist-like phenotype exists that satisfies the condition that growth rates in the two environments are equal ($\mu_{i,A} = \mu_{i,B}$).

We simulated the model dynamics for different values of $\bar{\mu}$, and plotted the temporal average of population in Fig 5. As a result, the continuous shift from a generalist-like strategy to specialist-like strategy was observed by decreasing $\bar{\mu}$. When $\bar{\mu}$ was larger than the branching point at $\bar{\mu} \approx 0.6$, the generalist-like strategy becomes dominant. When the value of $\bar{\mu}$ falls below the branching point, two types of phenotypes emerge. These phenotypes α and β were symmetric between environments A and B ($\mu_{\alpha,A} = \mu_{\beta,B}$ and $\mu_{\alpha,B} = \mu_{\beta,A}$). Near the branching point, the two dominant phenotypes showed little difference in growth rate between the two environments. As

$\bar{\mu}$ decreases, a specialist-like strategy adapted to only one of the environments becomes dominant. We also observed the shift from the generalist-like strategy to the two symmetric specialist-like strategies when we decreased b. As described in the previous section, we observed a shift from generalist to specialist dominance. However, introducing a continuous phenotype space reveals that this transition does not occur as a sharp transition, but rather unfolds gradually.

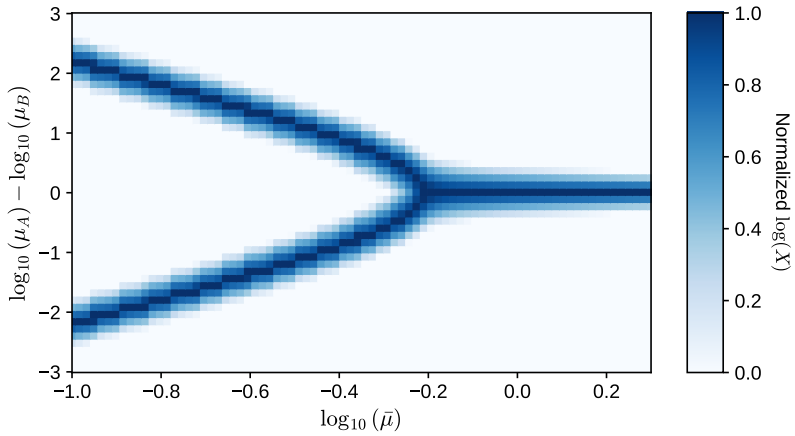

Fig 5. Transition of specialist and generalist. We simulated the dynamics with various $\bar{\mu}$ from $10^{-1.0}$ to $10^{0.3}$. We simulated the model up to $t = 2.0 \times 10^5$, and temporally averaged the populations from 20 nutrient supply events ago to the latest one. For each simulation, the logarithm of the average population in each bin, normalized from 0 to 1, is plotted. The parameters are set to $a = 0.01, b = 1, S_0 = 10$ and $\Delta\tau = 10$. The growth rate of each phenotype are set by Eq (10), where $m = 2, c = 0.2, g^{(0)} = m^{c(N+1)/2}$. varying in increments of 0.2. Phenotype switching occurs only in adjacent bins, and the phenotype switching probability is 10^{-4}. The x-axis represents the geometric mean, and the y-axis represents the difference between the growth rates of the two environments.

As in the setup above, the phenotype space satisfying Eq (3) is discretized into an $E - 1$ dimensional lattice, because the trade-off constraint effectively reduces the degrees of freedom by one. In the initial state, only phenotype i exists, which satisfies the condition that all growth rates in different environments are equal.

In a simulation with three environmental conditions, the dominance of generalists or specialists changed at a certain value of $\bar{\mu}$, as in the simulation with two environments. Fig 6 shows the temporal average of the population of each phenotype in one cycle after the system developed for a sufficiently long period to reach the steady population level on average. In Fig 6 (A) and (B), the three peaks stably coexist. Each peak is located at the position where the growth rates in two of the three environment are the same and are higher ($\mu_A = \mu_B > \mu_C$). Thus, these three phenotypes have specialist-like strategies being specialized in the two environments. Phenotypes that specialize in only one environmental condition were not dominant.

In the simulation with four environmental conditions, we observed two transition points. The first transition is from a generalist to phenotypes that specialize in three environmental conditions, and the second transition occurs at a lower $\bar{\mu}$, from phenotypes that specialize in three environmental conditions to phenotypes that specialize in two environmental conditions. As in the simulation with three environmental conditions, phenotypes that specialize in one environmental condition have never been dominant. The number of coexisting phenotypes never exceeds the

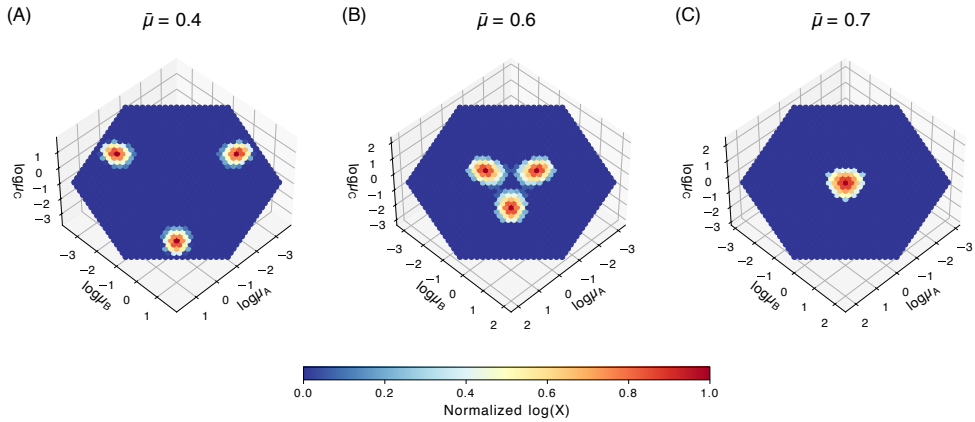

Fig 6. Examples of the simulation with $E = 3$. (A)The case with $\bar{\mu} = 0.4$. (B) $\bar{\mu} = 0.6$. (C) $\bar{\mu} = 0.7$. Each dot represents one phenotype. We simulated the population dynamics up to $t = 2.0 \times 10^5$. The heatmap represents the temporal average of the population from 30 nutrient supply events ago to the latest one. For each simulation, the logarithm of the mean population in each bin, normalized from 0 to 1, is plotted. Phenotypes with higher populations are marked in red. The parameters are set to $a = 0.01, b = 1, S_0 = 10$ and $\Delta\tau = 10$. The growth rate of each phenotypes in each environment was set as $\bar{\mu} \cdot 2^x, \bar{\mu} \cdot 2^y$ and $\bar{\mu} \cdot 2^z$, where $x + y + z = 0$ holds. Phenotypes can switch only between adjacent bins, with a transition probability of 10^{-4}.

number of environmental conditions E, as far as we have confirmed.

Discussion

In the present study, we developed a microbial population dynamics model under the feast-famine cycle to understand the possible mechanisms behind the diverse nutrient utilization strategies of microorganisms in temporally varying environments. In the model, each phenotype is defined by distinct growth rates on different nutrient types, and these rates are constrained by a resource-use trade-off that represents the underlying metabolic functional limitations. Nutrients are supplied to the system as discrete, stochastic events; once supplied, they are rapidly consumed by microbes, leading to a nutrient-depleted period. The alternation of nutrient-rich and nutrient-depleted conditions leads to the feast-famine cycle. Under the feast-famine cycle, cells face a trade-off between the growth rate in feast and death rate in famine.

In the simplest model with only three phenotypes and two types of nutrients, we demonstrated that the ratio between the growth rate in feast and death rate in famine determines whether the generalist or specialist phenotype is dominant. When a phenotype's growth-death ratio exceeds that of its competitors, it dominates; when it falls below theirs, it is outcompeted. In environments with fluctuating nutrient levels, cells require regulation of both growth under nutrient-rich conditions and survival under nutrient-poor conditions. In our model, this regulation is constrained by the growth-death trade-off (Eq (4)). Because a growth-death trade-off exists, cells must balance growth and survival by regulating their growth rate in each environment under the constraint of resource-use Eq (3), which leads to the emergence of generalist and specialist strategies.

In our simulations, we varied the value of the parameters $\bar{\mu}$ and b. These two

model parameters capture how external conditions and intrinsic physiology jointly affect the growth-death tatio The first parameter, $\bar{\mu}$, represents the geometric mean of the growth rates across nutrients. Cell growth depends not only on the amount of nutrients but also on various other environmental conditions such as temperature, pH, and anaerobic condition. $\bar{\mu}$ reflects the overall habitat favorability considering these conditions. Under higher $\bar{\mu}$, more favorable growth conditions dominate the generalist strategy. On the other hand, under lower $\bar{\mu}$, growth-restricted conditions, the specialists strategy will be dominant.

The second parameter, b, represents the strength of the growth-death trade-off. The larger its value, the more sharply the death rate increases with an increase in growth rate. This value is shaped by broad stress response systems that reallocate cellular resources from biosynthesis to protection from stresses, such as starvation. One example of a gene associated with the stress response is *rpoS*, which is a sigma factor for the general stress response, including the response to starvations. [30, 41–43]. Previous research has experimentally shown that deletion of *rpoS* in *E. coli* weakens the growth-death trade-off [34].

Notably, we observed that both strategies can be dominant depending on the strength of the growth-death trade-off, even though the metabolic utilization trade-off between different nutrients is fixed to a convex function. Previous theoretical studies have suggested that such convex trade-offs favor specialists and preclude the emergence of generalists. [14, 36, 37]. However, the situation in which only the functional form of the trade-off type sets the emerging strategy would be contradictory. Indeed, empirical studies have shown that changing only the frequency of environmental fluctuations can reverse which strategy has higher fitness [22, 25].

Changing the functional form of the resource-use tradeoff itself may be challenging for cells. Resource-use trade-offs are constrained by the metabolic function of cells. Such trade-offs derived from metabolism are expected to be rigid, as metabolic functions operate under biochemical and thermodynamic constraints, making metabolic innovations such as the acquisition of new metabolic pathways challenging [44]. Central carbon metabolism, such as glycolysis and the TCA cycle is evolutionarily conserved across a wide range of organisms [45, 46]. These metabolic pathways constrain key processes such as glycolysis/gluconeogenesis and carbon source co-utilization, and thus represent a key factor shaping resource-use trade-offs [9, 47, 48]. In contrast, the growth-death trade-off may exhibit greater plasticity than the resource-use trade-off. *rpoS* mutations are commonly found in laboratory and natural populations [31]. This suggests that the strength of the growth-death tradeoff may evolve through single mutations in regulatory genes.

Taken together, our results suggest that flexible regulation of stress tolerance can compensate for rigid metabolic constraints, allowing microbial communities to toggle between generalist and specialist strategies in response to temporally varying conditions, even when the underlying resource-use trade-off remains unchanged. This insight underscores the importance of considering multiple intersecting trade-offs when interpreting the ecological and evolutionary dynamics of nutrient utilization.

Acknowledgements

This work was supported by JSPS KAKENHI (Grant Numbers JP22H05403 and JP25H01390 to Y.H.; 22K21344 and 23K27164 to C. F.).

References

1. Brendan B. Larsen, Elizabeth C. Miller, Matthew K. Rhodes, and John J. Wiens. Inordinate Fondness Multiplied and Redistributed: The Number of Species on Earth and the New Pie of Life. *The Quarterly Review of Biology*, 92(3):229–265, September 2017.

2. William B. Whitman, David C. Coleman, and William J. Wiebe. Prokaryotes: The unseen majority. *Proceedings of the National Academy of Sciences*, 95(12):6578–6583, June 1998.

3. G F Gause. *The Struggle for Existence*.

4. Garrett Hardin. The Competitive Exclusion Principle. *Science*, 131(3409):1292–1297, April 1960.

5. Peter Chesson. Mechanisms of Maintenance of Species Diversity. *Annu. Rev. Ecol. Syst.*, 31(1):343–366, November 2000.

6. Silvia Brochet, Andrew Quinn, Ruben AT Mars, Nicolas Neuschwander, Uwe Sauer, and Philipp Engel. Niche partitioning facilitates coexistence of closely related honey bee gut bacteria. *eLife*, 10:e68583, July 2021.

7. Xiaoqian Annie Yu, Craig McLean, Jan-Hendrik Hehemann, David Angeles-Albores, Fuqing Wu, Artur Muszyński, Christopher H Corzett, Parastoo Azadi, Elizabeth B Kujawinski, Eric J Alm, and Martin F Polz. Low-level resource partitioning supports coexistence among functionally redundant bacteria during successional dynamics. *The ISME Journal*, 18(1):wrad013, January 2024.

8. Jamie M. Kneitel and Jonathan M. Chase. Trade-offs in community ecology: Linking spatial scales and species coexistence. *Ecology Letters*, 7(1):69–80, 2004.

9. David M Ekkers, Sergio Tusso, Stefany Moreno-Gamez, Marina C Rillo, and Oscar P Kuipers. Trade-Offs Predicted by Metabolic Network Structure Give Rise to Evolutionary Specialization and Phenotypic Diversification. *Molecular Biology and Evolution*, 39(6):msac124, June 2022.

10. Susan Soltau Kilham. Dynamics of Lake Michigan Natural Phytoplankton Communities in Continuous Cultures Along a Si:P Loading Gradient. *Can. J. Fish. Aquat. Sci.*, 43(2):351–360, February 1986.

11. Kyle F. Edwards, Christopher A. Klausmeier, and Elena Litchman. Evidence for a three-way trade-off between nitrogen and phosphorus competitive abilities and cell size in phytoplankton. *Ecology*, 92(11):2085–2095, 2011.

12. Matthew Scott, Carl W. Gunderson, Eduard M. Mateescu, Zhongge Zhang, and Terence Hwa. Interdependence of Cell Growth and Gene Expression: Origins and Consequences. *Science*, 330(6007):1099–1102, November 2010.

13. Sheng Hui, Josh M. Silverman, Stephen S. Chen, David W. Erickson, Markus Basan, Jilong Wang, Terence Hwa, and James R. Williamson. Quantitative proteomic analysis reveals a simple strategy of global resource allocation in bacteria. *Mol Syst Biol*, 11(1):784, February 2015.

14. Rodrigo Caetano, Yaroslav Ispolatov, and Michael Doebeli. Evolution of diversity in metabolic strategies. *eLife*, 10:e67764, August 2021.

15. Severin Josef Schink, Dimitris Christodoulou, Avik Mukherjee, Edward Athaide, Viktoria Brunner, Tobias Fuhrer, Gary Andrew Bradshaw, Uwe Sauer, and Markus Basan. Glycolysis/gluconeogenesis specialization in microbes is driven by biochemical constraints of flux sensing. *Molecular Systems Biology*, 18(1):e10704, January 2022.

16. Douglas J. Futuyma and Gabriel Moreno. The Evolution of Ecological Specialization. *Annual Review of Ecology and Systematics*, 19:207–233, 1988.

17. Jason P. Sexton, Jorge Montiel, Jackie E. Shay, Molly R. Stephens, and Rachel A. Slatyer. Evolution of Ecological Niche Breadth. *Annual Review of Ecology, Evolution, and Systematics*, 48(1):183–206, 2017.

18. Qicheng Xu, Philippe Vandenkoornhuyse, Ling Li, Junjie Guo, Chen Zhu, Shiwei Guo, Ning Ling, and Qirong Shen. Microbial generalists and specialists differently contribute to the community diversity in farmland soils. *Journal of Advanced Research*, 40:17–27, September 2022.

19. Joanne Clavel, Romain Julliard, and Vincent Devictor. Worldwide decline of specialist species: Toward a global functional homogenization? *Frontiers in Ecology and the Environment*, 9(4):222–228, 2011.

20. Anna Posfai, Thibaud Taillefumier, and Ned S. Wingreen. Metabolic Trade-Offs Promote Diversity in a Model Ecosystem. *Phys. Rev. Lett.*, 118(2):028103, January 2017.

21. Masashi Tachikawa. Fluctuation Induces Evolutionary Branching in a Mathematical Model of Ecosystems. *PLOS ONE*, 3(12):e3925, December 2008.

22. Tim F. Cooper and Richard E. Lenski. Experimental evolution with E. coli in diverse resource environments. I. Fluctuating environments promote divergence of replicate populations. *BMC Evolutionary Biology*, 10(1):11, January 2010.

23. Colin T. Kremer and Christopher A. Klausmeier. Coexistence in a variable environment: Eco-evolutionary perspectives. *Journal of Theoretical Biology*, 339:14–25, December 2013.

24. R. Kassen. The experimental evolution of specialists, generalists, and the maintenance of diversity. *Journal of Evolutionary Biology*, 15(2):173–190, 2002.

25. Vedant Sachdeva, Kabir Husain, Jiming Sheng, Shenshen Wang, and Arvind Murugan. Tuning environmental timescales to evolve and maintain generalists. *Proceedings of the National Academy of Sciences*, 117(23):12693–12699, June 2020.

26. Sujatha Srinivasan and Staffan Kjelleberg. Cycles of famine and feast: The starvation and outgrowth strategies of a marineVibrio. *J. Biosci.*, 23(4):501–511, October 1998.

27. Meinhard Simon, Hans-Peter Grossart, Bernd Schweitzer, and Helle Ploug. Microbial ecology of organic aggregates in aquatic ecosystems. *Aquatic Microbial Ecology*, 28(2):175–211, June 2002.

28. Jason Merritt and Seppe Kuehn. Frequency- and Amplitude-Dependent Microbial Population Dynamics during Cycles of Feast and Famine. *Phys. Rev. Lett.*, 121(9):098101, August 2018.

29. Yusuke Himeoka and Namiko Mitarai. Dynamics of bacterial populations under the feast-famine cycles. *Phys. Rev. Res.*, 2(1):013372, March 2020.

30. R. Hengge-Aronis. Survival of hunger and stress: The role of rpoS in early stationary phase gene regulation in E. coli. *Cell*, 72(2):165–168, January 1993.

31. Lucinda Notley-McRobb, Thea King, and Thomas Ferenci. rpoS Mutations and Loss of General Stress Resistance in Escherichia coli Populations as a Consequence of Conflict between Competing Stress Responses. *J Bacteriol*, 184(3):806–811, February 2002.

32. M. R. Maurizi. Proteases and protein degradation in Escherichia coli. *Experientia*, 48(2):178–201, February 1992.

33. David W. Erickson, Severin J. Schink, Vadim Patsalo, James R. Williamson, Ulrich Gerland, and Terence Hwa. A global resource allocation strategy governs growth transition kinetics of Escherichia coli. *Nature*, 551(7678):119–123, November 2017.

34. Elena Biselli, Severin Josef Schink, and Ulrich Gerland. Slower growth of Escherichia coli leads to longer survival in carbon starvation due to a decrease in the maintenance rate. *Molecular Systems Biology*, 16(6):e9478, June 2020.

35. Om Patange, Christian Schwall, Matt Jones, Casandra Villava, Douglas A. Griffith, Andrew Phillips, and James C. W. Locke. Escherichia coli can survive stress by noisy growth modulation. *Nat Commun*, 9(1):5333, December 2018.

36. Martijn Egas, Ulf Dieckmann, and Maurice W. Sabelis. Evolution Restricts the Coexistence of Specialists and Generalists: The Role of Trade-off Structure. *The American Naturalist*, 163(4):518–531, April 2004.

37. Elias Ehrlich, Lutz Becks, and Ursula Gaedke. Trait–fitness relationships determine how trade-off shapes affect species coexistence. *Ecology*, 98(12):3188–3198, 2017.

38. P. M. Vitousek and R. L. Sanford Jr. NUTRIENT CYCLING IN MOIST TROPICAL FOREST. *Annual Review of Ecology, Evolution, and Systematics*, 17(Volume 17,):137–167, November 1986.

39. Jue Wang, Esha Atolia, Bo Hua, Yonatan Savir, Renan Escalante-Chong, and Michael Springer. Natural Variation in Preparation for Nutrient Depletion Reveals a Cost–Benefit Tradeoff. *PLOS Biology*, 13(1):e1002041, January 2015.

40. Dominique Chu and David J. Barnes. The lag-phase during diauxic growth is a trade-off between fast adaptation and high growth rate. *Sci Rep*, 6(1):25191, April 2016.

41. Aurelia Battesti, Nadim Majdalani, and Susan Gottesman. The RpoS-Mediated General Stress Response in Escherichia coli*. *Annual Review of Microbiology*, 65(Volume 65, 2011):189–213, October 2011.

42. C R O'Neal, W M Gabriel, A K Turk, S J Libby, F C Fang, and M P Spector. RpoS is necessary for both the positive and negative regulation of starvation survival genes during phosphate, carbon, and nitrogen starvation in Salmonella typhimurium. *Journal of Bacteriology*, 176(15):4610–4616, August 1994.

43. Frieda Jørgensen, Steve Leach, Stephen J. Wilde, Angela Davies, Gordon S. A. B. Stewart, and Tom Humphrey. Invasiveness in chickens, stress resistance and RpoS status of wild-type Salmonella enterica subsp. enterica serovar Typhimurium definitive type 104 and serovar Enteritidis phage type 4 strains. *Microbiology*, 146(12):3227–3235, 2000.

44. Arren Bar-Even, Avi Flamholz, Elad Noor, and Ron Milo. Thermodynamic constraints shape the structure of carbon fixation pathways. *Biochimica et Biophysica Acta (BBA) - Bioenergetics*, 1817(9):1646–1659, September 2012.

45. Navdeep S. Chandel. Glycolysis. *Cold Spring Harb Perspect Biol*, 13(5):a040535, May 2021.

46. José M Peregrín-Alvarez, Chris Sanford, and John Parkinson. The conservation and evolutionary modularity of metabolism. *Genome Biol*, 10(6):R63, 2009.

47. Severin Josef Schink, Dimitris Christodoulou, Avik Mukherjee, Edward Athaide, Viktoria Brunner, Tobias Fuhrer, Gary Andrew Bradshaw, Uwe Sauer, and Markus Basan. Glycolysis/gluconeogenesis specialization in microbes is driven by biochemical constraints of flux sensing. *Mol Syst Biol*, 18(1):e10704, January 2022.

48. Sotaro Takano, Jean C C Vila, Ryo Miyazaki, Álvaro Sánchez, and Djordje Bajić. The Architecture of Metabolic Networks Constrains the Evolution of Microbial Resource Hierarchies. *Mol Biol Evol*, 40(9):msad187, August 2023.